
ОБЗОРНЫЕ
И ПРОБЛЕМНЫЕ СТАТЬИ

MOLECULAR MODELING IN STUDIES OF ION CHANNELS
AND THEIR MODULATION BY LIGANDS

© 2019 D. B. Tikhonov¹, *, B. S. Zhorov¹

¹*Sechenov Institute of Evolutionary Physiology and Biochemistry, Russian Academy of Sciences,
St. Petersburg, 194223, Russian Federation*

**e-mail: denistikhonov2002@yahoo.com*

Received July 9, 2019

Revised August 22, 2019

Accepted August 24, 2019

Ion channels constitute a diverse family of transmembrane proteins, which regulate flow of ions through cell membranes. The channels are involved in multiple physiological processes and they are targets for numerous naturally occurring toxins and medically important drugs. However, molecular details of the channel structure, mechanisms of action, and interaction with ligands are still debated. A reason for this is the shortage of atomic-level three dimensional structures. During last two decades significant contributions to the field have been made with indirect experimental approaches including mutagenesis, electrophysiology, and analysis of structure-function relations. Molecular modeling was applied to rationalize these experimental data in structural terms. Recent achievements of the X-ray crystallography and cryo-electron microscopy provide unambiguous solutions for many structural problems that were previously addressed by indirect and modeling studies. In this review we describe several examples of structural predictions that have been made by molecular modeling with the aim to rationalize indirect experimental data. We compare the models with recently published crystal and cryo-EM structures. A good agreement of many predictions with the later published experimental structures validates further employment of molecular modeling studies. Currently available and expected structures of principal ion channels and their complexes with ligands provide realistic templates for modeling homologous channels, their multiple variants, including disease-associated mutants, and docking drugs and toxins in the models. These studies are expected to provide high-quality predictions, which are necessary to design new channel-specific ligands and provide recommendations for personalized chemotherapy.

Keywords: sodium channels, calcium channels, glutamate-gated channels, molecular modeling, mechanism of block, channelopathies

DOI: 10.1134/S0869813919110116

Ion channels play fundamental roles in physiology. These proteins control passive ion transport through cell membranes. Fast ion permeation (millions of ions per second) changes membrane voltage and mediates rapid inflow of the second-messenger calcium ions, which regulate numerous intracellular processes. Ion channels are main elements of electrical signaling. They are responsible for reception, generation, propagation and transduction of signals in the nervous system. Synaptic plasticity, which represents cellular basis of learning and memory, is also associated with ion channels [1].

Ion channels are targeted by many drugs and naturally occurring toxins. More than 10% of all pharmacological agents regulate function of ion channels. Examples of ion channel ligands include, but are not limited to anesthetics and analgesics, antidepressants, anticonvulsants, antiarrhythmics and antihypertensive drugs. Therefore, development of potent and specific ion channel ligands is a primary goal of neuropharmacology. Despite decades of large efforts in academia and industry, our understanding of molecular basis of specific drugs action on ion channels is still incomplete. For example, molecular mechanisms of action of classical local anesthetics and anticonvulsants on voltage-gated sodium channel are still debated in physiological literature, see [2, 3]. There are two major causes of this situation. The first one is large variety of channel-forming proteins with different foldings, subunit compositions and functional states. This variety complicates investigations of ion channels structure, function and modulation because experimental data obtained for one channel class are poorly transferrable to another class. Secondly, membrane localization of ion channels has long prevented or complicated their isolation and purification, which is necessary for structural studies. Even nowadays representative structures are available for only a limited number of channel classes, although the rapid progress in the X-ray crystallography and cryo-electron microscopy (cryo-EM) provides increasingly large number of the channel structures. However, experimental structural studies are very complex and laborious and a new channel structure is usually published in a high-impact journal.

Molecular modeling approach. In lack of high-resolution experimental structures molecular modeling methods are usually applied to fill the gaps. Computational approaches, namely, molecular dynamics and Monte Carlo energy minimizations, employ experimental data on atom-interactions (force fields) to simulate behavior of molecular systems or predict energetically favorable structures [4]. However, the approximate nature of force fields and huge time required for computation at even modern supercomputers prevent hands-free predictions of ion channel folding. Therefore, in lack of crystal or cryo-EM structure of an ion channel, “homology modeling” approach can be used to predict its 3D structure [5, 6]. This approach is based on the assumption that the principal folding is conserved in a family of related proteins and therefore an available crystal or cryo-EM structure can be used as a template to predict structure of another channel from this family. Experimental data are also used to computationally predict ligand-channel complexes. Available data on structure-activity relationships and/or results of site-directed mutagenesis are used to reveal regions of ligand binding. Such information helps to build reliable models, which integrate results of indirect experiments obtained by different scientific groups with different experimental approaches. The models, in turn, provide structural rationale for the experimental data and help to design new experiments [7, 8].

The main problem with molecular models is that usually their precision and predictive potential are unknown until respective crystal or cryo-EM structure is obtained. In the last decades, this problem limited application of models of ion channels and their complexes with ligands in experimental studies. Recently, crystal and cryo-EM structures of the channels, which had been modeled in the past, become available. These experimental structures allow estimating precision of the modeling predictions. It is impossible to consider the large field of ion channels in this work. Therefore, we describe here several examples of our theoretical studies of so-called P-loop channels.

P-loop channels. P-loop channels constitute a superfamily of functionally and structurally different proteins, which have common folding of the pore-forming domain, but may have very different signal-recognition and modulatory domains. The family includes voltage-gated potassium, sodium and calcium channels, TRP channels, and channels gated by cyclic nucleotides and glutamate. All these channels are tetramers or pseudo-tetramers, in which the four subunits (repeats in case of eukaryotic sodium and calcium channels whose pore is formed by a single polypeptide) contribute to the pore domain a helix-loop-helix structural motif (Fig. 1A). The reentrant membrane loop (P-loop) between transmem-

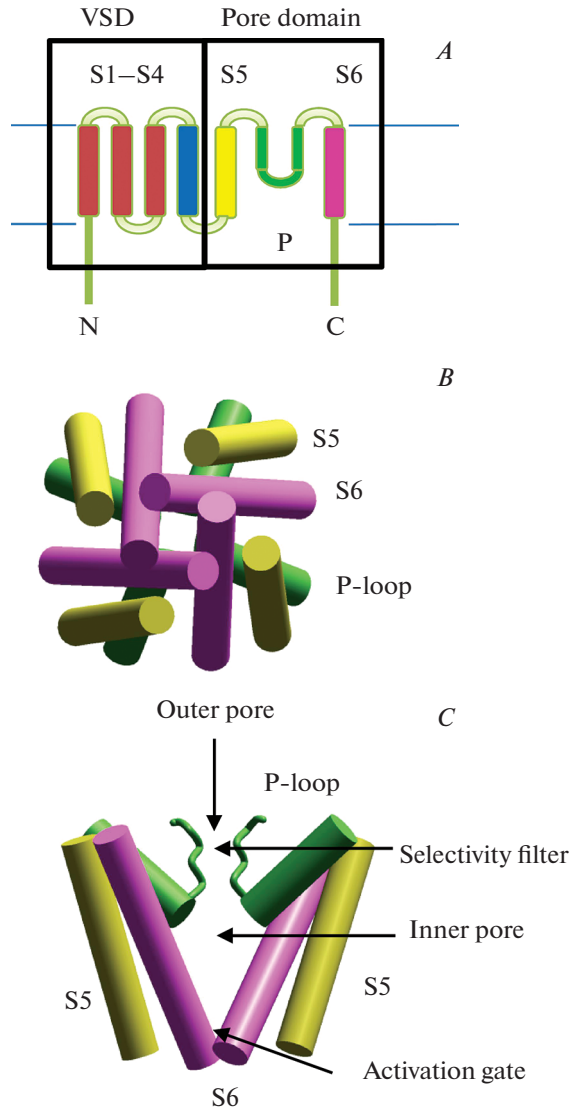


Fig. 1. General architecture of P-loop channels. *A*, Transmembrane topology of voltage-gated potassium channel subunit. The N-part forms voltage-sensing domain (VSD) with the voltage sensing segment S4. The C-part contributes to the pore domain and contains re-entrant membrane loop (P). *B* and *C*, extracellular (*B*) and side (*C*) views on the pore domain of potassium channel. Segments and main regions are labeled.

brane helices S5 and S6 harbors the selectivity filter. Interestingly, even membrane orientation of the pore domain can be different: in ionotropic glutamate receptors P-loops enter the membrane from the cytoplasm, whereas in other members they are located extracellularly. P-loops in sodium in calcium channels form a helix-loop-helix motif whereas other members of the superfamily contains only the first helix.

Models of sodium channels with outer pore-blocking toxins. Homology modeling of P-loop channels has become possible in 1998 when Roderick MacKinnon and colleagues

published pioneering crystal structure of a prokaryotic potassium channel KcsA [9]. Importance of this and several later resolved potassium channel structures for advancing our understanding of ion channels function at the atomic level was recognized by the Nobel Prize in chemistry in 2003. General organization of the pore domain revealed by these studies is shown in Figures 1*B*, *C*. A narrow selectivity filter formed by residues in the four loops divides the permeation pathway in two distinct regions, namely the inner pore and the outer pore.

An important example, which demonstrates the predictive power and limitations of the modeling approach based on indirect experimental data, is a series of theoretical studies of voltage-gated sodium channels whose outer pore is blocked by tetrodotoxin (TTX), saxitoxin (STX) and μ -conotoxins (μ CTX). The modeling was complicated by the fact that the outer pore of potassium channels is too narrow to accommodate even rather small molecules of TTX and STX, implying that the outer pore of sodium channels is substantially different from that in potassium channels. On the other hand, action of these toxins was addressed in many experimental studies, which provides patterns of specific toxins-channel interactions and even energetics of some interactions. Analysis of these interactions revealed a clockwise arrangement of repeats in pseudo-tetrameric sodium channels [10]. Rigid structures of TTX and STX allowed Lipkind and Fozzard to predict relative disposition of key TTX/STX sensing residues in the outer-pore region between the selectivity-filter DEKA ring (residues Asp, Glu, Lys and Ala from the four repeats) and the ring of so-called outer carboxylates [11]. However, to dock rigid TTX and STX in the outer pore, the authors suggested different disposition of the pore helices in the KcsA potassium channel, which was used as a template for modeling, and in the modeled sodium channel [12]. Later we have built a model with the same toxin-sensing residues, but kept the pore helices in KcsA-like disposition and used Monte Carlo energy minimizations that relaxed residues in the outer pore, allowing it to form rather wide region, which readily accommodates the toxins [13].

The next breakthrough was the crystal structure of a bacterial sodium channel NavAb [14]. Although the homotetrameric NavAb, as well as other prokaryotic sodium channels, NavRh [15] and NavMs [16], are not identical to sodium channels of eukaryotes, these structures revealed significant differences with potassium channels. In the latter channels the C-half of each P-loop has the second helix (P2) which is absent in potassium channels. Modeling studies did not reveal existence of the second helix in the region of the toxins binding that is an example of limitations of homology modeling approach in prediction of the secondary structure elements. Employment of the NavAb structure as a template for homology modeling allowed us to build a new model of TTX-bound channel Nav1.4 [17]. To elaborate the model, we introduced insertions/deletions (indels) in the selectivity-filter region in the aligned sequences of the homotetrameric prokaryotic and pseudo-heterotetrameric eukaryotic sodium channels (Fig. 2*A*). The indels were necessary to keep proper orientation of conserved structure-stabilizing residues and TTX-sensing residues in the 3D model.

The same model was used to rationalize interesting experimental data on the channel block by peptide KIIIA and other μ -conotoxins [18]. A peculiarity of the KIIIA action is an incomplete channel block. This was explained in the model where KIIIA binds between P-loops of repeats III and IV, does not occlude the outer pore, and leaves a path for TTX to reach the deeper located selectivity filter. Now we can compare these modeling predictions with recent structures of eukaryotic sodium channels [19, 20] and their complexes with TTX, STX and μ CTX [21]. The comparison is given in Fig. 2*B–E* and 3. Conserved 3D disposition of P-helices in potassium and sodium channels was correctly predicted. Indels in the sequence alignment of NavAb and eukaryotic channels were also correctly predicted (Fig. 2*A*). Disposition of TTX-sensing groups were predicted with a high precision (Fig. 2*B*, *C*). The binding mode of TTX/STX was correctly predicted in general, although

<i>A</i>	====P1====~SF~==P2=	===== S6 =====			
	41	51	2	11	21
KcsA	RAL WWSVETATTV	GYGDLYPVTL	WGRLVAVVV	MVAGITSFGL	VTAALATWF
Kvl.2	DAF WWAVVSMTTV	GYGDMVPTTI	GGKIVGSLC	AIAGVLTIAL	PVVFIVSNF
GluRI	NSL WFSLGAFMQQ	GC-DISPRSL	SGRIVGGVW	WFFTLIIISS	YTANLAAFL
NR1	SAM WFSWGVLLNS	GIGEGAPRSF	SARILGMVW	AGFAMIIVAS	YTANLAAFL
NavAB	GES FYTLFQVMTL	ESWSMGIVRP.	YAWVFFIFP	IFVVFVVMIN	LYVAIIVDA
Nav1.4	AWT FLCLFRLMLQ	DYW - EN LYQM.	SYMVFFIMV	IFLGSFYLIN	LILAVVAMA
	FHS FLIVFRALCG	E -W E -TMWD.	MCLAVYMMV	I IIGNLVMLN	LFLALLLSS
	GMG YLSLLQVSTF	KGW - MD IMYA.	YMYLYFVIF	IVFGAFTFLN	LFIGVIIDN
	GNS MICLFEITTS	AGW - D GLLLP.	KGITFFCSY	IILSFLVVVN	MYIAIILEN
Cav1.1	GFS MLTVYQCITM	EGWTDVLYWV.	WPWIYFVTL	ILLGSFFILN	LVLGVLSGE
	PQA LISVFQVLTG	EDWNSVMYNG.	LVCIYFIIL	FVCGNYILLN	VFLAIAVDN
	LSA MMSLFTVSTF	EGWPQLLYRA.	EMAIFFIIY	IILIAFFMMN	IFVGFVIPT
	PQA VLLLFRCATG	EAWQEILLAC.	FAYYYFISF	YMLCAFLIIN	LFVAVIMDN

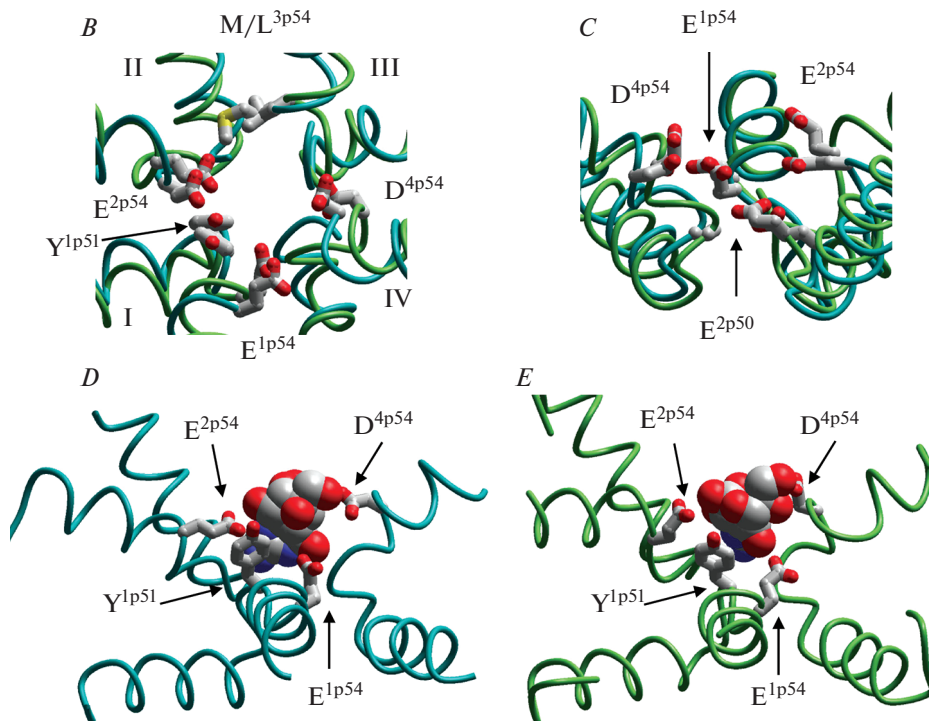


Fig. 2. Modeling of TTX binding in the outer pore of sodium channel. *A*, Sequence alignment of P-loops and inner helices of potassium, sodium, calcium and glutamate-gated channels. Key TTX-sensing residues estimated by mutational studies in the Nav1.4 are bold underlined. The insertions/deletions in the sequence alignment are proposed to reproduce in the model experimental data on TTX action. *B* and *C*, Extracellular (*B*) and side (*C*) views on superimposed structures of the model and cryo-EM structure (PDB code 6A95). Side chains of TTX-sensing residues are shown. *D* and *E*, Model (*D*) and cryo-EM structure (*E*) of TTX-bound channel. General orientation of TTX and main TTX-channel contacts match in the model and experimental structure.

some details of toxin-channel orientation do differ between the models and experimental structures (Fig. 2*D, E*). Asymmetric binding of μ CTX KIIIA against P2 helix of repeat III was correctly predicted (Fig. 3). It should be noted however, that exact KIIIA orientation

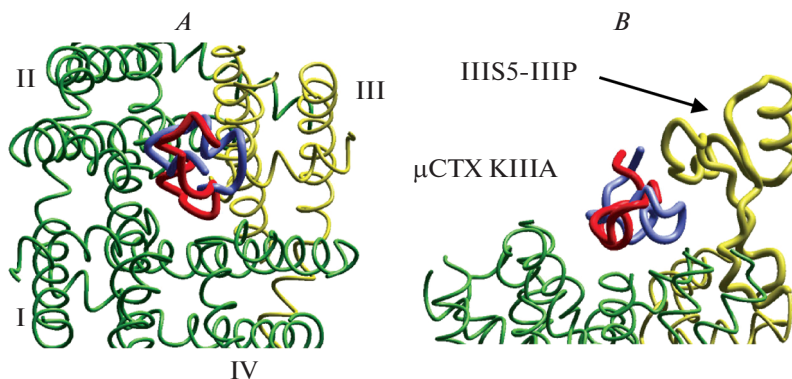


Fig. 3. Modeling μ CTX-KIIIA binding. Extracellular (*A*) and side (*B*) views on superimposed structures of the model and cryo-EM structure (PDB code 6J8E). Repeat III is yellow, The toxin backbone is blue in the model and red in the cryo-EM structure. The model correctly predicts KIIIA binding to P-loops in repeats III and IV and its significant shift from the pore axis (which allows TTX to reach the selectivity filter in KIIIA-bound channel). However, the toxin orientation in the channel is significantly different between the model and cryo-EM structure. Probable cause of this mismatch is the toxin interaction with extracellular III5-IIIIP external loop (*B*).

is substantially different in the model and in the experimental structure. Probable reason for this mismatch is the interaction of the toxin with long extracellular loops of the eukaryotic sodium channel (Fig. 3*B*), which were not considered in the models because the corresponding loops in available templates are short.

Thus, principal features of toxin binding were predicted correctly, but models and experimental structures do differ in some details. The major causes of these disagreements are the inherent limitations of the homology modeling approach that cannot account serious differences between the structural template and the modeled channel.

Models of sodium channels with the inner pore blockers. The inner pore region of sodium channels is targeted by important small-molecule drugs that include local anesthetics, antiarrhythmics and anticonvulsants. According to mutational data, charged local anesthetics, e.g. lidocaine, and electroneutral anticonvulsants, e.g. carbamazepine, share the same binding region inside the inner pore cavity, see [2]. Given that electrostatic interactions make significant contribution to ligand-protein energy in the low-dielectric membrane environment, such data is a challenging paradox in structure-activity relations of sodium channel ligands. To resolve this paradox, we elaborated models in which the ammonium group of a cationic ligand displaces a sodium ion from its binding site in the inner pore and occupies this site, whereas an electroneutral ligand chelates the sodium ion in this site [2]. In our models even bulky cationic groups of cocaine and quinidine do fit the sodium binding site in the inner pore. In complete agreement with our concept, the crystal structure of flecainide-bound NavAb shows the ligand's bulky cationic group that occupies the sodium binding site in the inner pore [22]. We are not aware of X-ray structures of ion channels with the pore-bound ligands, which are in direct contact with permeant ions. However, the key role of such contacts is demonstrated in a study of the hERG potassium channel with negatively charged activators [23].

Hydrophobic access pathway for drugs in the inner pore is another problem related to the action of LAs. This experimentally discovered pathway, which provides a slow drug access from membrane to the inner pore of the closed channel, is an important feature of the "modulated receptor" hypothesis that explains state-dependent action of LAs [24]. However, localization of this pathway was unknown. Our modeling study predicted that this

pathway, which we called a “sidewalk”, is located between S6 helices in repeats III and IV and the P-helix of repeat III [13]. Although the interface between S6 helices in potassium channel structures is too narrow, even modest deviations of the helices in our sodium channel model has made the sidewalk wide enough to let through some LAs [25]. This modeling prediction was confirmed in the crystal structure of the prokaryotic sodium channel NavAb where interfaces between S6 helices are dubbed “fenestrations” [14]. Indeed, sodium and potassium channels have slightly different spatial arrangement of transmembrane helices. Due to this difference sodium channel fenestrations are wide enough to let through molecules like LAs.

According to mutational data, LAs and related drugs strongly interact with residues in adjacent S6 helices that line the inner pore. Accordingly, in the classical scheme the ligands bind almost vertically with the aminogroup approaching the selectivity filter [26]. However, our computations predicted that closed-channel models lack room to accommodate LAs in such orientation. In the energetically optimal binding mode the drugs adopt horizontal orientation, the aromatic moiety extends into the repeat interface (sidewalk/fenestration), and the aminogroup at the pore axis approaches the selectivity filter to block permeation upon the channel opening [25]. In the crystal structure of the NavMs prokaryotic channel with a LA-like molecule PL1, only bromine atom is resolved [27], but its position in the fenestration completely agrees with our prediction (Fig. 4). Our prediction that some ligands, which block resting channels in the horizontal binding mode and directly interact with the fenestration-facing residues, is recently confirmed in the crystal structure of flecainide-bound NavAb [22]. Thus, localization of the hydrophobic access pathway between two S6 helices and P-helix, as well as binding mode of local anesthetics and related drugs in the pore, which were initially proposed in our models, is now generally accepted.

Ligands of the L-type calcium channel. Recently, the long-awaited cryo-EM structures of the Cav1.1 channel with important drugs (diltiazem, verapamil, dihydropyridine antagonist nifedipine and dihydropyridine agonist S-Bay k 8644) have been published [28]. In the cryo-EM structure, Cav1.1-bound diltiazem approaches the III/IV interface with the ligand ammonium group and the fused rings located in the inner pore. The cryo-EM structure confirms important aspects our Cav1.2 model with a diltiazem derivative in which the ligand ammonium group and bulky fused rings do bind in the inner pore and the methoxyphenyl ring protrudes into interface IIIP1/IIIS6/IVS6, which is proposed to constitute the drug access pathway from the membrane to the inner pore [29]. Our model was used to rationalize action of a photo-switchable derivative of diltiazem on the Cav1.2 channel [30].

In the cryo-EM structures, agonist S-Bay k 8644 and antagonist nifedipine bind in the III/IV repeat interface of Cav1.1. The agonist exposes its nitro group, the key determinant of the agonistic activity, to the permeation pathway, does not contact any channel residue and is available for interactions with the second hydration shell of a calcium ion, whereas the antagonist has a hydrophobic methoxy group in place of the agonist nitro group [28–30]. In our Cav1.2 models, dihydropyridine agonists and antagonists do bind in interface IIIP1/IIIS5/IIIS6/IVS6 and expose their hydrophilic or hydrophobic groups, respectively, to the permeation pathway; agonists are proposed to stabilize a permeant calcium ion, whereas antagonists would destabilize it [31–33]. In our models the ligands are closer to the pore axis than in the cryo-EM structures. Future studies are necessary to confirm or falsify the model-based proposal on the atomic mechanisms of action of dihydropyridine agonists and antagonists.

In one of the two cryo-EM structures of verapamil-bound Cav1.1, the ligand ammonium nitrogen is 5 Å from the closest to it calcium ion in the selectivity filter. A bigger distance of 6.3 Å between the same atoms is predicted in our model of devapamil-bound Cav1.2 [34]. In our model devapamil extends one of the methoxyphenyl rings into the

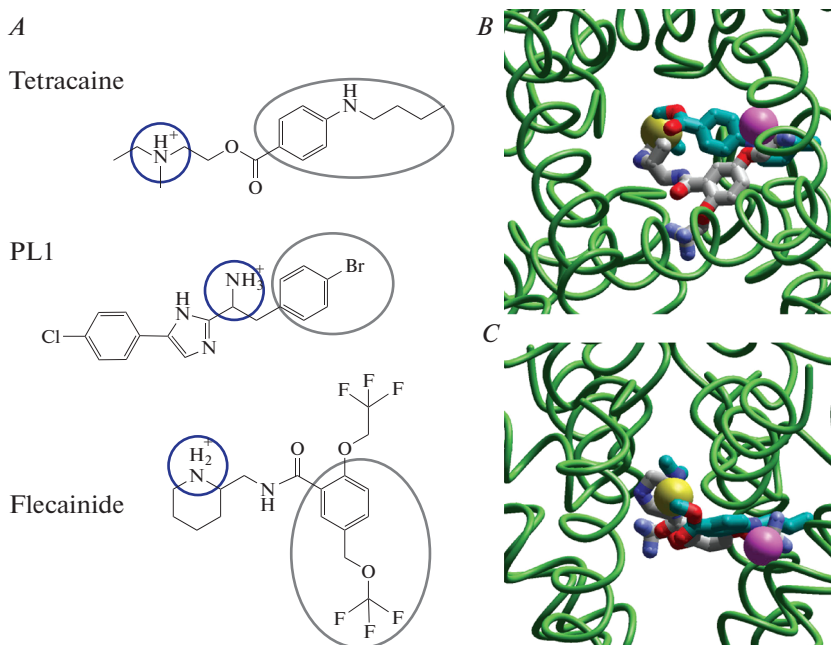


Fig. 4. Modeling of local anesthetics binding in the inner pore of sodium channels. *A*, Chemical structures. Charged amino groups that displace the ion from the selectivity filter and aromatic/hydrophobic moieties that bind in repeat interface are highlighted. *B* and *C*, Intracellular (*B*) and side (*C*) views of superimposition of tetracaine binding model with the crystal structure of unblocked channel (PDB code 5HVX), PL1 blocked channel NavMs (PDB ID 4P90) and flecainide-blocked channel NavAb (PDB code 6MVX). In the model, carbon atoms are cyan. The sodium ion in the ligand-free channel is shown as yellow sphere. The bromine atom of PL1 is magenta. Ligand binding mode is the same in all the structures.

III/IV repeat interface, an analogy with the LAs horizontal binding mode in sodium channels. In one of the cryo-EM structures a dimethoxyphenyl ring of verapamil also closely approaches the III/IV interface. Most importantly, in our model, but not in the cryo-EM structure, the nitrile group, a fingerprint of verapamil and other phenylalkylamines, interacts with the calcium ion in the selectivity filter to partially compensate repulsion between the ion and the charged ligand. The likely cause of the disagreement is detergent, which was used to extract the Cav1.1 channel from the membrane. In the cryo-EM structure one of the detergent molecules interacts with verapamil, approaches the calcium ion in the selectivity filter and prevents its contact with the nitrile group.

Altogether, in the cryo-EM structures of ligand-bound channel Cav1.1, less than half of ligand-sensing residues, which were previously identified in mutational studies, form specific contacts with the ligands [28]. Some of the earlier mutational studies may have revealed allosteric rather than direct ligand-channel interactions. However, the fact that no contacts with polar diltiazem- and verapamil-sensing residues are seen in the cryo-EM structures does not make sense in view of rich data on structure-activity relations of such ligands.

The disagreement between the mutational data, which reflect the channel block in physiological conditions, and cryo-EM structures that show deeply frozen ligand-channel complexes may be due to several factors. **Firstly**, each cryo-EM structure shows a single binding mode (two binding modes of verapamil), whereas dispersed ensembles of low-en-

ergy binding modes have been predicted with Monte Carlo energy minimizations [2] and molecular dynamics simulations [3, 35]. **Secondly**, physiological factors, such as membrane voltage, temperature, pH, and concentration of cations and anions are known to affect ligand action. These factors are lacking or may be misrepresented in the deeply frozen ligand-channel complexes. Binding modes of small Cav1.2 ligands, which act in micromolar concentrations, should be sensitive to these factors. **Thirdly**, the Cav1.1 channel is captured in a state with the activated voltage sensors, but closed activation gate. This structure is proposed to represent an inactivated state [28], but whether or not it corresponds to a physiological inactivated state is unknown.

Thus, the models and cryo-EM structures of ligand-bound calcium channels have both common and different features. The models are better consistent with indirect experimental data simply because these data were taken into consideration to select “physiological” binding modes among ensembles of predicted low-energy ligand-channel complexes. On the other hand, the cryo-EM structures represent long-awaited starting approximations for docking ligands in various Cav1.x channels and their disease-associated mutants. Such modeling studies are important for rationalizing available data on structure-activity relationships and design of new drugs.

Models of glutamate-gated channels with pore blockers. Another example of successful modeling predictions is the pore structure and binding of pore blockers in the glutamate-gated channels. The sequences of the pore-lining segments of glutamate receptor channels are close to those in potassium channels [36, 37]. This justified use of homology modeling with potassium channel crystal structures as templates. Molecular models provided different predictions about drug binding modes in the pore [38–41] and, in particular, proposed specific organization of the selectivity filter [38, 42]. In glutamate-gated channels, ion conductance, calcium permeability and binding of pore blockers are mainly controlled by so-called N/Q/R site, which is located at the P-loop turns [43]. The NMDA-type channels, which demonstrate large conductance, calcium permeability and are sensitive to various organic blockers, have asparagine in the N/Q/R site. In the AMPA-type subunits, this position can be occupied by glutamine or arginine. Presence of arginine in this site abolishes the calcium permeability and binding of cationic pore blockers. When the site contains glutamine, the channel properties are intermediate. In particular, NMDA-type channels are blocked by mono-cationic MK-801, ketamine and memantine. These mono-cationic blockers do not affect glutamine-containing AMPAR channels. However, polyamines, polyamine-containing toxins and long dicationic analogs of memantine and ketamine do block both NMDA and glutamine-containing AMPA receptor channels [43]. We proposed that the N/Q/R site residues are involved in intersubunit H-bonds that restrict conformational flexibility or the side chains. As a result, the carbonyl groups of asparagines face the pore, whereas the carbonyl groups of glutamine are directed away from the pore lumen and thus do not participate in coordination of permeant ions and binding of the channel blockers [38, 42]. Therefore, only long molecules, whose terminal groups can penetrate deeply into the selectivity filter region, can effectively block the pore. These models provided structural rationale for several structure-activity studies [44–46]. Comparison of the model with the recent structure [47] is given in Fig. 5A. It shows that the binding mode prediction was largely correct. Moreover, the cyclic organization of the selectivity filter also agrees with the predictions (Fig. 5, and C). The difference in the binding mode of argitoxin is stronger. In the models the toxin adopts a semifolded conformation due to intramolecular H-bonding. In the cryo-EM structure the toxin is almost extended. As a result the toxin penetrates completely the selectivity filter with its polyamine tail.

Perspectives of modeling approach. The above examples show that the homology modeling approach, which takes into account various experimental data, can predict important features of the channel structures and principal binding modes of ligands. The precision of predictions is mainly limited by the structural templates and used experimental datasets.

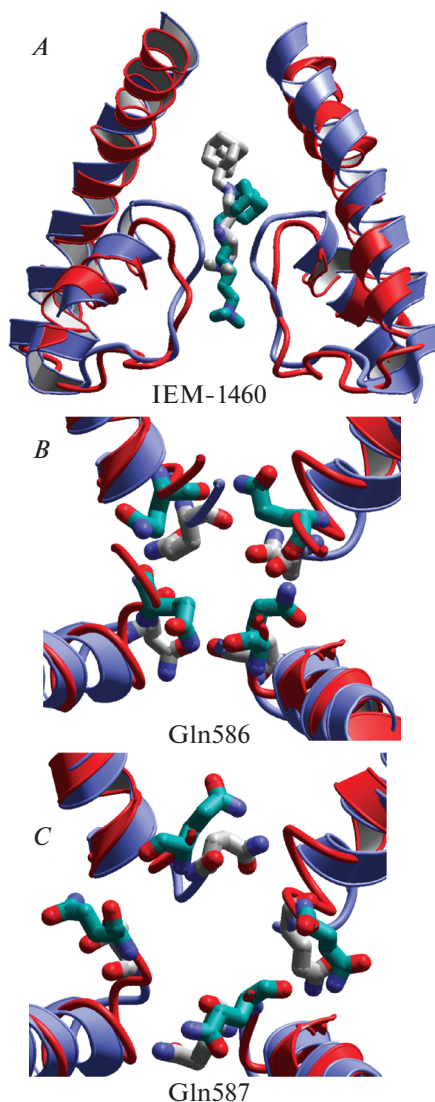


Fig. 5. Modeling binding of IEM-1460 in the AMPA receptor channel. *A*, Superimposition of the model and cryo-EM structure (PDB code 6DMO). Backbones in the model and experimental structure are red and violet, respectively. Carbons of IEM-1460 in the model are cyan. In both structures the adamantane group is located in the cavity, whereas terminal ammonium group penetrates into the selectivity filter. The only difference is some vertical shift of the ligand, which is caused by corresponding difference in the conformation at the P-loop turn. *B* and *C*, Intracellular views on rings formed by residues Gln586 (*B*) and Gln587 (*C*) in the selectivity filter.

This conclusion, which is based on comparison of our models with later published experimental structures, validates employments of the modeling approach for further studies. Certainly, impressive progress in experimental structural studies of ion channels provides unambiguous solutions for many important problems, which previously were addressed by indirect studies interpreted with homology modeling. More experimental structures are expected in future. This should shift the focus of modeling studies towards more specific

questions. Indeed, it is unlikely that structures of many ion channels in different organisms, their multiple mutants, and complexes with various ligands will be resolved experimentally in the foreseen future. Below are some problems that can be addressed with molecular modeling.

Drug design. At first sight, the number of approved drugs seems larger than that of target channels. However, if we consider all channel isoforms in different organisms and different states and their naturally occurring mutations, for example, disease-associated mutations and mutations in insects that adapted to tolerate insecticides, the number of channels is much larger than that of practically used ligands. For example, some mutations cause drug insensitivity, a well-known phenomenon of largely unknown mechanisms. This creates a large room for further applications of molecular modeling, which is now based on much more adequate structural templates.

Before crystal and cryo-EM structures of eukaryotic P-loop channels became available, homology modeling helped to address general location of the ligand binding site, rationalize experimental data, explain effects of mutations on ligand action, generate testable hypothesis on residues contributing to ligand receptors, and guide further experimental studies. However, precision of homology models was too low to predict quantitatively potency of different drugs. Cryo-EM and crystal structures present reliable starting approximations to dock various ligands with the aims to quantitatively analyze structure-activity relationships and assist medicinal chemists in development of new more selective drugs. There is no shortage of paradoxes in structure-activity relations, which call for explanations in structural terms. For example, the above mentioned cryo-EM structures of the Cav1.1 channel with different ligands [28] do not show ligand contacts with many ligand-sensing residues that have been determined in previous mutational studies and do not completely explain important peculiarities of structure-activity relations of ligands.

Channelopathies. Public databases describe thousands of genetic mutations in human ion channels, which are associated with inherited diseases called channelopathies. For example, ClinVar database lists over 1,500 variants of gene SCN5A, which encodes the α_1 subunit of cardiac sodium channel Nav1.5 [48]. Many of these variants are associated with arrhythmias, including long-QT syndrome type 3 (LQT3), Brugada syndrome, cardiac conduction disease, sick sinus syndrome and atrial standstill [49–51]. Loss-of-function Nav1.5 mutations may enhance the channel inactivation, impair steady-state activation, decelerate recovery from inactivation or decrease current density. In contrast, gain-of-function mutations of Nav1.5, which underlie LQT3, often cause opposite biophysical changes. Mutations in other sodium channels are also associated with severe diseases. Thus, many mutations in gene SCN1A, which encodes neuronal sodium channel Nav1.1, are associated with genetic epilepsy syndromes [52]. Genetic mutations of the skeletal muscle sodium channel Nav1.4 are associated with such diseases as potassium-aggravated myotonia, paramyotonia congenita, hyperkalemic periodic paralysis, hypokalemic periodic paralysis, and a form of congenital myasthenic syndrome [53]. Loss-of function mutations in Nav1.7, which is expressed in sensory and autonomic neurons, result in congenital insensitivity to pain, whereas gain-of-function mutations cause such pain syndromes as inherited erythromelalgia, paroxysmal extreme pain disorder, and small-fibre neuropathy [54]. Mutations in the Nav1.8 and Nav1.9 channels are associated, respectively, with small-fibre neuropathy and congenital insensitivity to pain.

According to a unified loss-of-function hypothesis for epilepsy syndromes caused by genetic changes in the Nav1.1 channels, mild impairment predisposes to febrile seizures, intermediate impairment leads to generalized epilepsy with febrile seizures plus, and severe loss of function causes severe myoclonic epilepsy of infancy [55]. Many Nav1.1 mutations, which are described in the ClinVar database, are mapped in the 3D structure of Cav1.1 channel [56], but understanding mechanistic effects of specific mutations on the channel

gating awaits molecular modeling focused on state-dependent contacts of wild-type and mutated residues.

Attempts to explain in structural terms how channelopathy-associated mutations affect functional properties of P-loop channels are rare. One example concerns data that lysine substitution of asparagine in the middle of helix IS6 in Nav1.5 and glutamate substitution of asparagine at the C-end of helix IVS6 are associated with LQTS syndrome [57]. Independently of this publication, we predicted that these asparagine residues, which are exceptionally conserved in S6 helices of sodium and calcium channels, form H-bonds with polar residues at the C-ends of neighboring S6 helices in the open, but not closed structures [58]. Our prediction of the state-dependent H-bonds is consistent with recent structures of sodium and calcium channels. It explains why substitutions of the asparagines with longer and more flexible residues, which would fortify the intersegment open-state H-bonds, cause gain-of-function of the Nav1.5 channel manifested as the LQT syndrome [57].

Another example is structural interpretation of a channelopathy mutation R518C in the VSD-II cytoplasmic N-end of the Cav1.2 channel [59]. The mutation, which is re-discovered in the Almazov National Medical Research Centre (St Petersburg), is associated with Timothy syndrome (TS), a very rare multisystem disorder. Previously, TS-associated Cav1.2 mutations R518C/H, as well as mutations G402S and G406R in helix IS6 of the pore domain were demonstrated to decelerate voltage-dependent inactivation [60–62]. However, structural mechanisms of these effects were unknown. To understand the mechanisms, the three Cav1.2 variants have been modeled using cryo-EM structures of presumably inactivated channel Cav1.1 [63] and crystal structures of the open and closed channel NavAb [64]. Steered Monte Carlo energy minimizations were used to transfer the Cav1.2 pore domain from the presumably inactivated state, which is inherited from the Cav1.1 template, to the open and closed states, which are seen in the NavAb crystal structures. Computations predicted that conformational changes in VSD-II upon its deactivation would propagate through the cytoplasmic linker I/II to the C-end of helix IS6 and initiate its transition to the closed-gate conformation. Helix IS6 would bend at flexible glycines G402 and G406, facilitating the activation gate closure. Mutations R518C/H would retard the I/II linker shift and thus transition of IS6 to the closed-gate conformation. Mutations G406R and G402S would stabilize the open state and thus also resist the pore closure. This study provided a mechanistic rationale for deceleration of the voltage-dependent inactivation caused by three TS-associated mutations and suggests targets for further studies of calcium channelopathies.

Towards personalized chemotherapy of channelopathies. A recent study describes a group of 15 patients with the same clinical phenotype (LQT3), which was associated with different mutations in the Nav1.5 channel [65]. The patients demonstrated different response to mexiletine, which is used to treat this type of arrhythmia. Biophysical studies of the mutated channels revealed different effects of mexiletine on conformation of VSD-III and electrophysiological characteristics of the channel. These data were used to build a statistical model that successfully predicted response to mexiletine for seven of eight other LQT3 patients whose Nav1.5 variants were electrophysiologically studied. However, structural mechanisms of different effects of mexiletine on the channel variants are unknown. This and many other intriguing experimental data on channelopathies, as well as large sets of data on ligand action on wildtype channels and their variants, call for interpretation in structural terms. Molecular modeling will contribute to such interpretations.

ACKNOWLEDGEMENT

Supported by grant to BSZ (17-04-00549) from the Russian Foundation for Basic Research.

REFERENCE

1. *Hille B.* Ion channels of excitable membranes. 3rd ed. Sunderland, Mass.: Sinauer. 2001.
2. *Tikhonov D.B., Zhorov B.S.* Mechanism of sodium channel block by local anesthetics, antiarrhythmics, and anticonvulsants. *J. Gen. Physiol.* 149(4): 465–481. 2017.
3. *Nguyen P.T., DeMarco K.R., Vorobyov I., Clancy C.E., Yarov-Yarovsky V.* Structural basis for antiarrhythmic drug interactions with the human cardiac sodium channel. *Proc. Natl. Acad. Sci. U. S. A.* 116(8): 2945–2954. 2019.
4. *Sledz P., Caflisch A.* Protein structure-based drug design: From docking to molecular dynamics. *Curr. Opin. Struct. Biol.* 48: 93–102. 2018.
5. *Muhammed M.T., Aki-Yalcin E.* Homology modeling in drug discovery: Overview, current applications, and future perspectives. *Chem. Biol. Drug Des.* 93(1): 12–20. 2019.
6. *Xiang Z.* Advances in homology protein structure modeling. *Curr. Protein Pept. Sci.* 7(3): 217–227. 2006.
7. *Giorgetti A., Carloni P.* Molecular modeling of ion channels: structural predictions. *Curr. Opin. Chem. Biol.* 7(1): 150–156. 2003.
8. *Sigg D.* Modeling ion channels: Past, present, and future. *J. Gen. Physiol.* 144(1): 7–26. 2014.
9. *Doyle D.A., Morais Cabral J., Pfuetzner R.A., Kuo A., Gulbis J.M., Cohen S.L., Chait B.T., MacKinnon R.* The structure of the potassium channel: Molecular basis of K⁺ conduction and selectivity. *Science.* 280(5360): 69–77. 1998.
10. *Dudley S.C., Jr., Chang N., Hall J., Lipkind G., Fozzard H.A., French R.J.* mu-conotoxin GIIIA interactions with the voltage-gated Na⁺ channel predict a clockwise arrangement of the domains. *J. Gen. Physiol.* 116(5): 679–690. 2000.
11. *Lipkind G.M., Fozzard H.A.* A structural model of the tetrodotoxin and saxitoxin binding site of the Na⁺ channel. *Biophys. J.* 66(1): 1–13. 1994.
12. *Lipkind G.M., Fozzard H.A.* KcsA crystal structure as framework for a molecular model of the Na⁺ channel pore. *Biochemistry.* 39(28): 8161–8170. 2000.
13. *Tikhonov D.B., Zhorov B.S.* Modeling P-loops domain of sodium channel: Homology with potassium channels and interaction with ligands. *Biophys. J.* 88(1): 184–197. 2005.
14. *Payandeh J., Scheuer T., Zheng N., Catterall W.A.* The crystal structure of a voltage-gated sodium channel. *Nature.* 475(7356): 353–358. 2011.
15. *Zhang X., Ren W., DeCaen P., Yan C., Tao X., Tang L., Wang J., Hasegawa K., Kumasaka T., He J., Wang J., Clapham D. E., Yan N.* Crystal structure of an orthologue of the NaChBac voltage-gated sodium channel. *Nature.* 486(7401): 130–134. 2012.
16. *McCusker E.C., Bagnieris C., Naylor C.E., Cole A.R., D'Avanzo N., Nichols C.G., Wallace B.A.* Structure of a bacterial voltage-gated sodium channel pore reveals mechanisms of opening and closing. *Nat. Commun.* 3: 1102. 2012.
17. *Tikhonov D.B., Zhorov B.S.* Architecture and Pore Block of Eukaryotic Voltage-Gated Sodium Channels in View of NavAb Bacterial Sodium Channel Structure. *Mol. Pharmacol.* 82(1): 97–104. 2012.
18. *Korkosh V.S., Zhorov B.S., Tikhonov D.B.* Folding similarity of the outer pore region in prokaryotic and eukaryotic sodium channels revealed by docking of conotoxins GIIIA, PIIIA, and KIIIA in a NavAb-based model of Nav1.4. *J. Gen. Physiol.* 144(3): 231–244. 2014.
19. *Shen H., Zhou Q., Pan X., Li Z., Wu J., Yan N.* Structure of a eukaryotic voltage-gated sodium channel at near-atomic resolution. *Science.* 355(6328). 2017.
20. *Yan Z., Zhou Q., Wang L., Wu J., Zhao Y., Huang G., Peng W., Shen H., Lei J., Yan N.* Structure of the Nav1.4-beta1 complex from Electric Eel. *Cell.* 170(3): 470–482 e11. 2017.
21. *Shen H., Li Z., Jiang Y., Pan X., Wu J., Cristofori-Armstrong B., Smith J.J., Chin Y.K.Y., Lei J., Zhou Q., King G.F., Yan N.* Structural basis for the modulation of voltage-gated sodium channels by animal toxins. *Science.* 362(6412). 2018.
22. *Gamal El-Din T.M., Lenaeus M.J., Zheng N., Catterall W.A.* Fenestrations control resting-state block of a voltage-gated sodium channel. *Proc. Natl. Acad. Sci. U. S. A.* 115(51): 13111–13116. 2018.
23. *Schewe M., Sun H., Mert U., Mackenzie A., Pike A.C.W., Schulz F., Constantin C., Vowinkel K.S., Conrad L.J., Kiper A. K., Gonzalez W., Musinszki M., Tegtmeier M., Pryde D.C., Belabed H., Nazare M., de Groot B.L., Decher N., Fakler B., Carpenter E.P., Tucker S.J., Baukrowitz T.* A pharmacological master key mechanism that unlocks the selectivity filter gate in K⁺ channels. *Science.* 363(6429): 875–880. 2019.
24. *Hille B.* Local anesthetics: Hydrophilic and hydrophobic pathways for the drug-receptor reaction. *J. Gen. Physiol.* 69(4): 497–515. 1977.
25. *Bruhova I., Tikhonov D.B., Zhorov B.S.* Access and binding of local anesthetics in the closed sodium channel. *Mol. Pharmacol.* 74(4): 1033–1045. 2008.
26. *Yarov-Yarovsky V., McPhee J.C., Idsvoog D., Pate C., Scheuer T., Catterall W.A.* Role of amino acid residues in transmembrane segments IS6 and IIS6 of the Na⁺ channel alpha subunit in voltage-dependent gating and drug block. *J. Biol. Chem.* 277(38): 35393–35401. 2002.

27. *Bagneris C., DeCaen P.G., Naylor C.E., Pryde D.C., Nobeli I., Clapham D.E., Wallace B.A.* Prokaryotic NavMs channel as a structural and functional model for eukaryotic sodium channel antagonism. *Proc. Natl. Acad. Sci. U. S. A.* 111(23): 8428–8433. 2014.
28. *Zhao Y., Huang G., Wu J., Wu Q., Gao S., Yan Z., Lei J., Yan N.* Molecular Basis for Ligand Modulation of a Mammalian Voltage-Gated Ca(2+) Channel. *Cell.* 177(6): 1495–1506 e12. 2019.
29. *Tikhonov D.B., Zhorov B.S.* Molecular modeling of benzothiazepine binding in the L-type calcium channel. *J. Biol. Chem.* 283(25): 17594–17604. 2008.
30. *Fehrentz T., Huber F.M.E., Hartrampf N., Bruegmann T., Frank J.A., Fine N.H.F., Malan D., Danzl J.G., Tikhonov D.B., Sumser M., Sasse P., Hodson D.J., Zhorov B.S., Klocker N., Trauner D.* Optical control of L-type Ca²⁺ channels using a diltiazem photoswitch. *Nat. Chem. Biol.* 14(8): 764–767. 2018.
31. *Yamaguchi S., Zhorov B.S., Yoshioka K., Nagao T., Ichijo H., Adachi-Akq̄hane S.* Key roles of Phe(1112) and Ser(1115) in the pore-forming IIS5–S6 linker of L-type Ca²⁺ channel alpha(1C) subunit (Ca(V)1.2) in binding dihydropyridines and action of Ca²⁺ channel agonists. *Mol. Pharmacol.* 64(2): 235–248. 2003.
32. *Tikhonov D.B., Zhorov B.S.* Structural Model for Dihydropyridine Binding to L-type Calcium Channels. *J. Biol. Chem.* 284(28): 19006–19017. 2009.
33. *Zhorov B.S., Folkman E.V., Ananthanarayanan V.S.* Homology model of dihydropyridine receptor: Implications for L-type Ca²⁺ channel modulation by agonists and antagonists. *Arch. Biochem. Biophys.* 393(1): 22–41. 2001.
34. *Cheng R.C.K., Tikhonov D.B., Zhorov B.S.* Structural Model for Phenylalkylamine Binding to L-type Calcium Channels. *J. Biol. Chem.* 284(41): 28332–28342. 2009.
35. *Buyan A., Sun D., Corry B.* Protonation state of inhibitors determines interaction sites within voltage-gated sodium channels. *Proc. Natl. Acad. Sci. U. S. A.* 115(14): E3135–E3144. 2018.
36. *Wo Z.G., Oswald R.E.* Unraveling the modular design of glutamate-gated ion channels. *Trends Neurosci.* 18(4): 161–168. 1995.
37. *Wood M.W., VanDongen H.M., VanDongen A.M.* Structural conservation of ion conduction pathways in K channels and glutamate receptors. *Proc. Natl. Acad. Sci. U. S. A.* 92(11): 4882–4886. 1995.
38. *Tikhonov D.B.* Ion channels of glutamate receptors: Structural modeling. *Mol. Membr. Biol.* 24(2): 135–147. 2007.
39. *Tikhonov D.B., Mellor J.R., Usherwood P.N., Magazanik L.G.* Modeling of the pore domain of the GLUR1 channel: Homology with K⁺ channel and binding of channel blockers. *Biophys. J.* 82(4): 1884–1893. 2002.
40. *Tikhonova I.G., Baskin II, Palyulin V.A., Zefirov N.S.* 3D-model of the ion channel of NMDA receptor: Qualitative and quantitative modeling of the blocker binding. *Dokl. Biochem. Biophys.* 396: 181–186. 2004.
41. *Kaczor A.A., Kijkowska-Murak U.A., Kronbach C., Unverferth K., Matosiuk D.* Modeling of glutamate GluR6 receptor and its interactions with novel noncompetitive antagonists. *J. Chem. Inf. Model.* 49(4): 1094–1104. 2009.
42. *Tikhonov D.B., Zhorov B.S., Magazanik L.G.* Intersegment hydrogen bonds as possible structural determinants of the N/Q/R site in glutamate receptors. *Biophys. J.* 77(4): 1914–1926. 1999.
43. *Traynelis S.F., Wollmuth L.P., McBain C.J., Menniti F.S., Vance K.M., Ogden K.K., Hansen K.B., Yuan H., Myers S.J., Dingledine R.* Glutamate receptor ion channels: Structure, regulation, and function. *Pharmacol. Rev.* 62(3): 405–496. 2010.
44. *Andersen T.F., Tikhonov D.B., Bolcho U., Bolshakov K., Nelson J.K., Pluteanu F., Mellor I.R., Egebjerg J., Stromgaard K.* Uncompetitive antagonism of AMPA receptors: Mechanistic insights from studies of polyamine toxin derivatives. *J. Med. Chem.* 49(18): 5414–5423. 2006.
45. *Bolshakov K.V., Kim K.H., Potapjeva N.N., Gmiro V.E., Tikhonov D.B., Usherwood P.N., Mellor I.R., Magazanik L.G.* Design of antagonists for NMDA and AMPA receptors. *Neuropharmacology.* 49(2): 144–155. 2005.
46. *Nelson J.K., Frolund S.U., Tikhonov D.B., Kristensen A.S., Stromgaard K.* Synthesis and biological activity of argiotoxin 636 and analogues: Selective antagonists for ionotropic glutamate receptors. *Angew. Chem. Int. Ed. Engl.* 48(17): 3087–3091. 2009.
47. *Twomey E.C., Yelshanskaya M.V., Vassilevski A.A., Sobolevsky A.I.* Mechanisms of Channel Block in Calcium-Permeable AMPA Receptors. *Neuron.* 99(5): 956–968. 2018.
48. *Landrum M.J., Lee J.M., Riley G.R., Jang W., Rubinstein W.S., Church D.M., Maglott D.R.* ClinVar: Public archive of relationships among sequence variation and human phenotype. *Nucleic Acids Res.* 42(Database issue): D980–985. 2014.
49. *Amin A.S., Asghari-Roodsari A., Tan H.L.* Cardiac sodium channelopathies. *Pflugers Arch.* 460(2): 223–237. 2010.
50. *Kapplinger J.D., Tester D.J., Alders M., Benito B., Berthet M., Brugada J., Brugada P., Fressart V., Guerchicoff A., Harris-Kerr C., Kamakura S., Kyndt F., Koopmann T.T., Miyamoto Y., Pfeiffer R., Pollevick G.D., Probst V., Zumhagen S., Vatta M., Towbin J.A., Shimizu W., Schulze-Bahr E., Antzelevitch C., Salisbury B.A., Guicheney P., Wilde A.A., Brugada R., Schott J.J., Ackerman M.J.* An

- international compendium of mutations in the SCN5A-encoded cardiac sodium channel in patients referred for Brugada syndrome genetic testing. *Heart Rhythm*. 7(1): 33–46. 2010.
51. *Brugada P.* Brugada syndrome: More than 20 years of scientific excitement. *J. Cardiol*. 67: 215–220. 2016.
 52. *Catterall W.A., Kalume F., Oakley J.C.* Nav1.1 channels and epilepsy. *J. Physiol*. 588(Pt 11): 1849–1859. 2010.
 53. *Jurkat-Rott K., Holzherr B., Fauler M., Lehmann-Horn F.* Sodium channelopathies of skeletal muscle result from gain or loss of function. *Pflugers Arch*. 460(2): 239–248. 2010.
 54. *Bennett D.L., Woods C.G.* Painful and painless channelopathies. *Lancet Neurol*. 13(6): 587–599. 2014.
 55. *Catterall W.A., Sodium Channel Mutations and Epilepsy*, in *Jasper's Basic Mechanisms of the Epilepsies*. *Noebels J.L., Avoli M., Rogawski M.A., Olsen R.W., Delgado-Escueta A.V.*, Editors. Bethesda (MD). 2012.
 56. *Huang W., Liu M., Yan S.F., Yan N.* Structure-based assessment of disease-related mutations in human voltage-gated sodium channels. *Protein Cell*. 8(6): 401–438. 2017.
 57. *Kato K., Makiyama T., Wu J., Ding W.G., Kimura H., Naiki N., Ohno S., Itoh H., Nakanishi T., Matsuura H., Horie M.* Cardiac channelopathies associated with infantile fatal ventricular arrhythmias: From the cradle to the bench. *J. Cardiovasc. Electrophysiol*. 25(1): 66–73. 2014.
 58. *Tikhonov D.B., Bruhova I., Garden D.P., Zhorov B.S.* State-dependent inter-repeat contacts of exceptionally conserved asparagines in the inner helices of sodium and calcium channels. *Pflugers Arch*. 467(2): 253–266. 2015.
 59. *Korkosh V.S., Kiselev A.M., Mikhaylov E.N., Kostareva A.A., Zhorov B.S.* Atomic Mechanisms of Timothy Syndrome-Associated Mutations in Calcium Channel Cav1.2. *Front. Physiol*. 10: 335. 2019.
 60. *Boczek N.J., Ye D., Jin F., Tester D.J., Huseby A., Bos J.M., Johnson A.J., Kanter R., Ackerman M.J.* Identification and Functional Characterization of a Novel CACNA1C-Mediated Cardiac Disorder Characterized by Prolonged QT Intervals With Hypertrophic Cardiomyopathy, Congenital Heart Defects, and Sudden Cardiac Death. *Circ. Arrhythm. Electrophysiol*. 8(5): 1122–1132. 2015.
 61. *Dick I.E., Joshi-Mukherjee R., Yang W., Yue D.T.* Arrhythmogenesis in Timothy Syndrome is associated with defects in Ca(2+)-dependent inactivation. *Nat. Commun*. 7: 10370. 2016.
 62. *Barrett C.F., Tsien R.W.* The Timothy syndrome mutation differentially affects voltage- and calcium-dependent inactivation of Cav1.2 L-type calcium channels. *Proc. Natl. Acad. Sci. U. S. A.* 105(6): 2157–2162. 2008.
 63. *Wu J., Yan Z., Li Z., Qian X., Lu S., Dong M., Zhou Q., Yan N.* Structure of the voltage-gated calcium channel Ca(v)1.1 at 3.6 Å resolution. *Nature*. 537(7619): 191–196. 2016.
 64. *Lenaeus M.J., Gamal El-Din T.M., Ing C., Ramanadane K., Pomes R., Zheng N., Catterall W.A.* Structures of closed and open states of a voltage-gated sodium channel. *Proc. Natl. Acad. Sci. U. S. A.* 114(15): E3051–E3060. 2017.
 65. *Zhu W., Mazzanti A., Voelker T.L., Hou P., Moreno J.D., Angsutararux P., Naegle K. M., Priori S.G., Silva J.R.* Predicting Patient Response to the Antiarrhythmic Mexiletine Based on Genetic Variation. *Circ. Res*. 124(4): 539–552. 2019.

МЕТОДЫ МОЛЕКУЛЯРНОГО МОДЕЛИРОВАНИЯ В ИЗУЧЕНИИ СТРОЕНИЯ ИОННЫХ КАНАЛОВ И ИХ МОДУЛЯЦИИ ЛИГАНДАМИ

Д. Б. Тихонов^{а, *}, Б. С. Жоров^а

^аИнститут эволюционной физиологии и биохимии им. И.М. Сеченова РАН,
Санкт-Петербург, Россия

*E-mail: denistikhonov2002@yahoo.com

Ионные каналы представляют собой разнообразное семейство трансмембранных белков, которые регулируют поток ионов через клеточные мембраны. Они вовлечены в многочисленные физиологические процессы и являются мишенями для разнообразных природных токсинов и фармакологических препаратов. Однако молекулярные детали структур каналов, механизмы их работы и взаимодействия с лигандами все еще обсуждаются. Одной из причин этого является нехватка трехмерных структур атомарного разрешения. В течение последних двух десятилетий значительный вклад в эту область внесли косвенные экспериментальные подходы, включая мутагенез, электрофизиологию и анализ структурно-функциональных связей в рядах лигандов. Молекулярное моделирование широко применялось для структурной интерпретации этих экспериментальных данных. Последние достижения рентгеновской кристаллографии и криоэлектрон-

ной микроскопии дают однозначные решения многих структурных проблем, которые ранее решались только косвенными и модельными исследованиями. В этом обзоре описывается несколько примеров структурных предсказаний, которые были сделаны с помощью молекулярного моделирования с целью объяснения косвенных экспериментальных данных. Мы сравниваем модели с недавно опубликованными экспериментальными структурами. Хорошее согласие многих предсказаний с более поздними опубликованными экспериментальными структурами подтверждает перспективы дальнейшего использования молекулярных модельных исследований. Имеющиеся в настоящее время и ожидаемые структуры основных ионных каналов и их комплексов с лигандами обеспечивают реалистичные шаблоны для моделирования каналов, их множественных вариантов, в том числе связанных с каналопатиями, и для предсказания связывания фармакологических препаратов и токсинов. Эти исследования, как ожидается, обеспечат высококачественные прогнозы, которые необходимы для разработки новых специфичных для канала лигандов и рекомендаций по персонализированной терапии.

Ключевые слова: натриевые каналы, кальциевые каналы, глутамат-активируемые каналы, молекулярное моделирование, механизмы блокады, каналопатии

ЦИТИРОВАТЬ:

Тихонов Д.Б., Жоров Б.С. Методы молекулярного моделирования в изучении строения ионных каналов и их модуляции лигандами. Рос. физиол. журн. им. И.М. Сеченова. 105(11): 1333–1348.

DOI: 10.1134/S0869813919110116

TO CITE THIS ARTICLE:

Tikhonov D.B., Zhorov B.S. Molecular Modeling in Studies of Ion Channels and Their Modulation by Ligands. Russian Journal of Physiology. 105(11): 1333–1348.

DOI: 10.1134/S0869813919110116